ResearchGate

See discussions, stats, and author profiles for this publication at: https://www.researchgate.net/publication/260369155

Electrochemical behaviour of mixed d metal–iron containing Wells–Dawson sandwich-type complexes: [(FeOH2)(2)M-2(X2W15O56)(2)](n-) and [(MOH2)(2)Fe-2(X2W15O56)(2)](n-) (M = Cr-III,...

ARTICLE *in* ELECTROCHIMICA ACTA · APRIL 2014

Impact Factor: 4.5 · DOI: 10.1016/j.electacta.2014.01.151

CITATION
1

READS
146

7 AUTHORS, INCLUDING:

Floriant Doungmene
Université Paris-Sud 11
6 PUBLICATIONS **36** CITATIONS
SEE PROFILE

Pablo Aparicio
TUM CREATE
10 PUBLICATIONS **53** CITATIONS
SEE PROFILE

Xavier López
Universitat Rovira i Virgili
67 PUBLICATIONS **1,599** CITATIONS
SEE PROFILE

All in-text references underlined in blue are linked to publications on ResearchGate, letting you access and read them immediately.

Available from: Xavier López
Retrieved on: 22 January 2016

Electrochimica Acta 125 (2014) 674–682

Contents lists available at ScienceDirect

Electrochimica Acta

journal homepage: www.elsevier.com/locate/electacta

Electrochemical behaviour of mixed d metal-iron containing Wells-Dawson sandwich-type complexes: $[(FeOH_2)_2M_2(X_2W_{15}O_{56})_2]^{n-}$ and $[(MOH_2)_2Fe_2(X_2W_{15}O_{56})_2]^{n-}$ (M = Cr^{III}, Mn^{III}, Mn^{II}, Co^{II}, Ni^{II}, Cu^{II}, Zn^{II}, X = As^V or P^V and n = 12 or 14)

Floriant Doungmene[a], Pablo A. Aparicio[b], Joseline Ntienoue[c], Charyle S. Ayingone Mezui[c], Pedro de Oliveira[a], Xavier López[b,*], Israël M. Mbomekallé[a,c,*]

[a] Université Paris-Sud, Laboratoire de Chimie-Physique, Equipe d'Electrochimie et de Photoélectrochimie, UMR 8000 CNRS, Orsay, F-91405, France
[b] Departament de Química Física i Inorgànica, Universitat Rovira i Virgili, Marcel·li Domingo s/n, 43007 Tarragona, Spain
[c] Université de Versailles St. Quentin, Institut Lavoisier de Versailles, UMR 8180 CNRS, Versailles, F-78035, France

ARTICLE INFO

Article history:
Received 24 November 2013
Received in revised form 17 January 2014
Accepted 26 January 2014
Available online 10 February 2014

Keywords:
Polyoxometalates
Electrochemistry
DFT calculations

ABSTRACT

An innovative study on the electrochemical behaviour of mixed d metal-iron containing Wells-Dawson sandwich-type complexes $[(FeOH_2)_2M_2(X_2W_{15}O_{56})_2]^{14-}$ and $[(MOH_2)_2Fe_2(X_2W_{15}O_{56})_2]^{14-}$ (with M = Cr^{III}, Mn^{II}, Mn^{III}, Co^{II}, Ni^{II}, Cu^{II} or Zn^{II} and X = P^V or As^V) was carried out. These complexes have a four-centre equatorial metal cluster constituted of two Fe atoms and two atoms of another metal. The Fe^{III} centres are either in an external position, $[(FeOH_2)_2M_2]$, or in an internal position, $[M_2(OH_2)_2Fe_2]$. Experimental methods (cyclic voltammetry and controlled potential coulometry) and theoretical calculations (density functional theory) allowed us to determine and analyse the redox potential values associated with the reduction of the Fe^{III} centres in these species. The influence of the position of the Fe^{III} centres, the nature of the metal centre M and the electron density distribution in the tetranuclear cluster (either $[(FeOH_2)_2M_2]$ or $[(MOH_2)_2Fe_2]$) have been studied and rationalised in order to account for the observed behaviours. The data suggest that the most stable isomers are those where Fe^{III} centres are internally-located, $[(MOH_2)_2Fe_2]$. Consequently, their reduction is more difficult than those having externally-located Fe^{III} isomers, $[(FeOH_2)_2M_2]$. Some experimental results revealed a few exceptions to this rule which have not been rationalised yet.

© 2014 Elsevier Ltd. All rights reserved.

1. Introduction

Combined theoretical-experimental studies can give a highly detailed view of the behaviour and distribution of electrons in molecules. In the case of the complex poly-metallic systems of the present work, the role of quantum chemistry is capital to understand and corroborate the experimental findings at the molecular level. In the present study on sandwich-type polyoxometalates, with several transition metals competing for the incoming electrons, the quantum chemical calculations have largely helped to understand the distribution of valence electrons localised in the equatorial plane of the molecules. Also, the molecular orbital view is a well-accepted language among chemists, both theoretical and experimental, to communicate chemical information in a simple though explanatory way. In this regard, computations represent the most straightforward path to achieve this goal. A versatile and attracting subclass of polyoxometalates (POMs) is constituted by the sandwich-type POMs (STPs). They are based on Keggin-like ($[XW_9O_{33}]^{n-}$, $[XW_9O_{34}]^{n-}$ and $[XW_{10}O_{36}]^{n-}$, X = As^V, P^V, Si^{IV}, ...) or Wells-Dawson-like ($[X_2W_{15}O_{56}]^{12-}$, X = As^V or P^V) fragments that incorporate metal oxide clusters in the so-called equatorial region.[1–3] Such clusters usually contain two, three or four metal centres, the latter two being the most common situations.[4–51] Irrespective of the constitutive fragments, the equatorial region features the same connectivity and properties when the metal oxide cluster contains the same number of metal centres.[31] The main differences observed between STPs based on the Keggin or the Wells-Dawson architecture are the overall molecular charge and size. The physicochemical properties of this subclass of molecules are still under investigation by virtue of their versatility and potential applications in different fields such as catalysis,[20] molecular magnetism,[14] etc.[52–56]

* Corresponding authors.
E-mail addresses: javier.lopez@urv.cat (X. López), israel.mbomekalle@u-psud.fr (I.M. Mbomekallé).

0013-4686/$ – see front matter © 2014 Elsevier Ltd. All rights reserved.
http://dx.doi.org/10.1016/j.electacta.2014.01.151

For the Keggin STPs, the first synthesised complexes were the $[(MOH_2)_2M_2(PW_9O_{34})_2]^{10-}$ (M = Co^{II}, Cu^{II}, Zn^{II}) anions.[5] The Co^{II} derivative is also one of the most studied complexes because of its potential application as a water oxidation catalyst.[57,58] The first characterized mixed-valence transition metal compound was $[(MnOH_2)_2Mn_2(PW_9O_{34})_2]^{n-}$, reported by Pope and co-workers,[59] where the Mn atoms have a mixture of +II and +III oxidation states. This compound exhibits magnetic properties and has been a model system for the study of electron exchange interactions within the internal cluster.[13] Another well-studied structure and the first Keggin-derived STP containing just trivalent transition metal ions in the equatorial region is $[(FeOH_2)_2Fe_2(PW_9O_{34})_2]$, a system that was tackled by density functional theory (DFT) calculations by Romo *et al.* [60] This compound is able to catalyse the oxidation of internal alkenes with H_2O_2, but it is an inefficient catalyst for primary alkenes. Depending on the nature of the transition metal atoms constituting the equatorial region, these systems may feature magnetic properties.[11,14,61] The first example of a mixed-metal sandwich-type complex described by Wasfi *et al.* in 1987 [8] proceeded by a one pot synthesis and contained two different d metal centres in its central cluster. Later on Santiago Reinoso *et al.* have described the first heterometallic 3d-4f derivatives based on the B-α-$[GeW_9O_{34}]^{10-}$, that contained either $[\{Ce^{III}(H_20)_2\}_2Mn^{III}{}_2]$ [62] or $[\{Ce^{III}(OAc)\}Cu^{II}{}_3(H_20)]$ as central clusters.[63]

As for the Keggin-based STPs, the first synthesized Wells-Dawson-based complexes were the $[(MOH_2)_2M_2(P_2W_{15}O_{56})_2]^{16-}$ (M = Co^{II}, Cu^{II}, Zn^{II}) anions.[6] The first compound with trivalent metal cations was $[(FeOH_2)_2Fe_2(P_2W_{15}O_{56})_2]^{12-}$, synthesised and characterised by Hill and co-workers.[20] Sometimes one or two of the transition metal atoms is substituted by alkali atoms such as Na^+. Other structures have also been synthesised, like the following complexes: $[(NaOH_2)_2Fe_2(X_2W_{15}O_{56})_2]^{16-}$ and $[(NaOH_2)(FeOH_2)Fe_2(X_2W_{15}O_{56})_2]^{14-}$, where X = As^V or P^V; [35] $[(NaOH_2)_2Cu_2(X_2W_{15}O_{56})_2]^{18-}$, where X = As^V or P^V; [40] $[(NaOH_2)_2M_2(As_2W_{15}O_{56})_2]^{18-}$ with M = Ni^{II}, Mn^{II} and Mn^{III}; [64,65] $[(NaOH_2)_2Co_2(P_2W_{15}O_{56})_2]^{18-}$ and $[(NaOH_2)(MOH_2)M_2(P_2W_{15}O_{56})_2]^{17-}$, where M = Co^{II} and Mn^{II}. [30,42] Substitution of the Na^+ ions by a different "d" metallic centre has led to a new class of STPs, the mixed metal complexes: $[(NiOH_2)_2Fe_2(P_2W_{15}O_{56})_2]^{14-}$, $[(ZnOH_2)_2Fe_2(X_2W_{15}O_{56})_2]^{14-}$ with X = As^V or P^V and $[(NaOH_2)_2Mn_2(As_2W_{15}O_{56})_2]$. [16–31,39,64,65]

The aim of the present work is to study the electrochemical behaviour of the mixed d metal-iron containing Wells-Dawson sandwich-type complexes $[(FeOH_2)_2M_2(X_2W_{15}O_{56})_2]^{14-}$ and $[(MOH_2)_2Fe_2(X_2W_{15}O_{56})_2]^{14-}$ (M = Cr^{III}, Mn^{III}, Mn^{II}, Co^{II}, Ni^{II}, Zn^{II}, Cu^{II} and X = P^V or As^V) by means of experimental measurements and DFT calculations. A representation of these compounds can be found in Fig. 1.

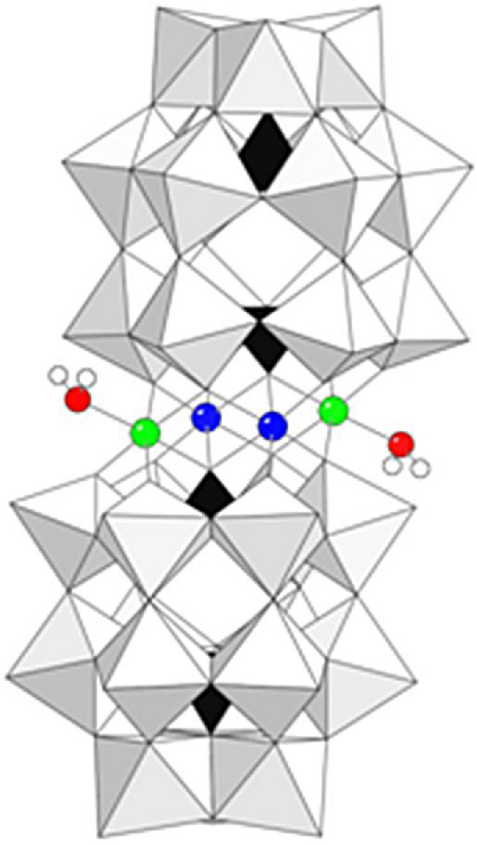

Fig. 1. Wells-Dawson-based sandwich-type structure, with the cluster of four metal atoms and two water molecules (ball-and-stick) between two $[X_2W_{15}O_{56}]$ fragments (polyhedra). Typically, green and blue spheres are referred to as external and internal positions, respectively.

2. Experimental Section

2.1. Chemicals

Pure water obtained with a RiOs 8 unit followed by a Millipore-Q Academic purification set was used throughout. All reagents were of high-purity grade and were used as purchased without further purification. H_2SO_4 (Sigma Aldrich), CH_3COOH (Carlo Erba), $Li_2SO_4.H_2O$ (Alfa Aesar) and $LiCH_3COO.2H_2O$ (Fluka) were commercial products. The composition of the various media was as follows: for pH 3.0, 0.5 M $Li_2SO_4 + H_2SO_4$; for pH 6.0, 1.0 M $LiCH_3COO + CH_3COOH$. Detailed procedures and full characterisation of $[(FeOH_2)_2M_2(As_2W_{15}O_{56})_2]^{n-}$, $[(MOH_2)_2Fe_2(As_2W_{15}O_{56})_2]^{n-}$ (M = Cr^{III}, Mn^{II}, Mn^{III}, Co^{II}, Cu^{II} and $n = 14$ or 13), $[(NaOH_2)_2Co_2(As_2W_{15}O_{56})_2]^{18-}$ and $[(NaOH_2)_2Zn_2(As_2W_{15}O_{56})_2]^{18-}$ will be published elsewhere. We have not been able to isolate pure samples of the compounds $[(Cr^{III}OH_2)_2Fe_2(As_2W_{15}O_{56})_2]^{12-}$ and $[(Mn^{III}OH_2)_2Fe_2(As_2W_{15}O_{56})_2]^{12-}$ so far. Pure samples of $[(NaOH_2)_2Fe_2(As_2W_{15}O_{56})_2]^{16-}$ and $[(NaOH_2)_2M_2(As_2W_{15}O_{56})_2]^{n-}$ (M = Mn^{II}, Mn^{III}, Ni^{II}, Cu^{II} and $n = 16$ or 18), $[(FeOH_2)_2M_2(As_2W_{15}O_{56})_2]^{14-}$ and $[(MOH_2)_2Fe_2(As_2W_{15}O_{56})_2]^{14-}$ (M = Zn^{II} and Ni^{II}) were obtained by following previously reported synthesis protocols.[35,64–66] Starting materials necessary for these syntheses, $[As_2W_{18}O_{62}]^{6-}$ and $[As_2W_{15}O_{56}]^{12-}$, were prepared according to published procedures.[67,68] Sample purity was confirmed by IR and cyclic voltammetry. Tungstophosphates STPs, $[(MOH_2)_2Fe_2(P_2W_{15}O_{56})_2]^{n-}$ and $[(FeOH_2)_2M_2(P_2W_{15}O_{56})_2]^{n-}$, have the same structural and physical properties as their tungstoarsenate analogues cited above. An obvious difference in their electrochemical behaviours consists in slightly more negative redox potentials for P containing POMs compared to As containing ones.

The stability of different polyanions in solution as a function of pH and time was studied by monitoring their UV-visible spectra at least over 6 h. Such duration is long enough for the electrochemical characterisation of these compounds. At the end of this study, two pH values were selected for the electrochemical studies: pH 3.0 and pH 6.0.

The IR spectra were recorded on a Nicolet 6700 FT Spectrometer driven by a PC with the OMNIC E.S.P. 5.2 software. The UV-visible spectra were recorded on a Perkin-Elmer Lambda 19 spectrophotometer using 2.5×10^{-5} M solutions of the relevant

polyanion. Matched 10.000 mm optical path quartz cuvettes were used.

Electrochemical data (cyclic voltammetry (CV) and controlled potential coulometry (CPC)) was obtained using an EG & G 273 A potentiostat driven by a PC with the M270 software. A one-compartment cell with a standard three-electrode configuration was used for cyclic voltammetry experiments. The reference electrode was a saturated calomel electrode (SCE) and the counter electrode a platinum gauze of large surface area; both electrodes were separated from the bulk electrolyte solution via fritted compartments filled with the same electrolyte. The working electrode was a 3 mm OD glassy carbon disc or a *c.a.* $10 \times 10 \times 2\,mm^3$ plate (GC, Le Carbone Lorraine, France). The pre-treatment of this electrode before each experiment has been described elsewhere.[69] The polyanion concentration was 2×10^{-4} M. Prior to each experiment, solutions were de-aerated thoroughly for at least 30 min with pure Ar. A positive pressure of this gas was maintained during subsequent work. All cyclic voltammograms were recorded at a scan rate of 10 mV s^{-1} unless otherwise stated. All experiments were performed at room temperature, which is controlled and fixed for the lab at 20 °C. Results were very reproducible from one experiment to another and slight variations observed over successive runs are attributed to the uncertainty associated with the detection limit of our equipment (potentiostat, hardware and software) rather than to the working electrode pre-treatment or to possible variations in temperature.

2.2. Calculations

Density functional theory (DFT) calculations have been carried out using the Gaussian 09 suite of programs.[70] The geometries of all the structures were fully optimised in conditions of no protonation and their energies obtained within the constraints of the C_{2h} symmetry point group. Reduction energies (REs) were computed as purely electronic $E^{red}-E^{ox}$ energy differences. We applied the B3LYP hybrid functional [71] and double-ζ + polarization basis sets: 6-31G(d,p), for H and O atoms and Hay-Wadt with Los Alamos National Laboratory pseudopotentials [72] (LANL2DZ) for metal atoms. The calculations include the Polarizable Continuum Model [73] (PCM) to account for the solvent effects of water ($\varepsilon = 78.4$), which is essential for a correct description of REs. The solute cavity was created using a scaled van der Waals surface with atomic radii corresponding to the Universal Force Field parameters, a Karplus/York smoothing algorithm and Lebedev-Laikov grids of ~5 points per $Å^2$. We applied the spin-unrestricted formalism to electronically open-shell molecules. Atomic spin populations (ASPs) were obtained by means of the Mulliken formula.

3. Results and discussion

3.1. Experimental part

The electrochemical experiments were carried out solely with the dodeca-octotungstodiarsenate derivatives $[As_2W_{18}O_{62}]^{6-}$. The species containing P as the central heteroatom have not been studied experimentally in this work. In fact, the influence of the nature of the heteroatom, either As or P, on the electrochemical response is the same for all metallic clusters such as $[(MOH_2)_2Fe_2]$ or $[(FeOH_2)_2M_2]$ (with M = Cr^{III}, Mn^{II}, Mn^{III}, Fe^{III}, Co^{II}, Ni^{II}, Cu^{II} or Zn^{II}), namely a slight cathodic shift ($\Delta E < 0.020$ V) of the redox waves when As is replaced by P. This behaviour has been described in several papers and is not the purpose of the present study. [39,40,66,74] The STP molecules selected for the present work were tested in two media, where both compounds are stable enough: 1.0 M $LiCH_3COO + CH_3COOH$/pH 6.0, where the influence of protonation is less obvious, and 0.5 M $Li_2SO_4 + H_2SO_4$/pH 3.0 where protonation has a greater effect on the redox behaviour of these STPs. We concentrated on the peak potentials associated with the reduction of the Fe^{III} centres depending on the nature and on the position of the M metal cations in the central cluster. The cathodic peak potential values associated with the Fe^{III} centres, $E_{pc}(Fe_1)$ and $E_{pc}(Fe_2)$, obtained by CV using glassy carbon working electrodes either in 1.0 M $LiCH_3COO + CH_3COOH$/pH 6.0 or in 0.5 M $Li_2SO_4 + H_2SO_4$/pH 3.0 are compiled in Table 1.

By and large, two distinct situations are envisaged: 1) the compound $[(NaOH_2)_2Fe_2(As_2W_{15}O_{56})_2]^{16-}$ is the original structure characterised by a central metallic cluster $[(NaOH_2)_2Fe^{III}{}_2]$, in which the two Fe^{III} centres are internally located. Each Fe^{III} ion is bound to six oxygen atoms of the oxo-tungstic scaffold. The two externally located sodium ions are then selectively replaced by

Table 1
Cathodic peak potentials (E_{pc} vs SCE/V) for the first and/or the second single-electron reduction step of Fe^{III} centres either in 1.0 M $LiCH_3COO + CH_3COOH$/pH 6.0 or in 0.5 M $Li_2SO_4 + H_2SO_4$/pH 3.0.

pH 6					
	$E_{pc}(Fe_1)$	$E_{pc}(Fe_2)$		$E_{pc}(Fe_1)$	$E_{pc}(Fe_2)$
$[(NaOH_2)_2Fe^{III}{}_2]$	−0.220	−0.330	–	–	–
$[(Zn^{II}OH_2)_2Fe^{III}{}_2]$	−0.150	−0.270	$[(Fe^{III}OH_2)_2Zn^{II}{}_2]$	−0.180	−0.280
$[(Cu^{II}OH_2)_2Fe^{III}{}_2]$	−0.130 [a]		$[(Fe^{III}OH_2)_2Cu^{II}{}_2]$	−0.130 [a]	
$[(Ni^{II}OH_2)_2Fe^{III}{}_2]$	−0.200	−0.310	$[(Fe^{III}OH_2)_2Ni^{II}{}_2]$	0.000	−0.100
$[(Co^{II}OH_2)_2Fe^{III}{}_2]$	−0.090	−0.220	$[(Fe^{III}OH_2)_2Co^{II}{}_2]$	−0.090	−0.260
$[(Mn^{II}OH_2)_2Fe^{III}{}_2]$	−0.160	−0.280	$[(Fe^{III}OH_2)_2Mn^{II}{}_2]$	−0.160	−0.270
$[(Mn^{III}OH_2)_2Fe^{III}{}_2]$ [c]	–	–	$[(Fe^{III}OH_2)_2Mn^{III}{}_2]$	−0.150	−0.270
$[(Cr^{III}OH_2)_2Fe^{III}{}_2]$ [c]	–	–	$[(Fe^{III}OH_2)_2Cr^{III}{}_2]$	−0.290 [b]	
pH 3					
	$E_{pc}(Fe_1)$	$E_{pc}(Fe_2)$		$E_{pc}(Fe_1)$	$E_{pc}(Fe_2)$
$[(NaOH_2)_2Fe^{III}{}_2]$	−0.090	−0.200			
$[(Zn^{II}OH_2)_2Fe^{III}{}_2]$	−0.080	−0.190	$[(Fe^{III}OH_2)_2Zn^{II}{}_2]$	−0.070	−0.190
$[(Cu^{II}OH_2)_2Fe^{III}{}_2]$	−0.130[a]		$[(Fe^{III}OH_2)_2Cu^{II}{}_2]$	−0.120 [a]	
$[(Ni^{II}OH_2)_2Fe^{III}{}_2]$	−0.060	−0.190	$[(Fe^{III}OH_2)_2Ni^{II}{}_2]$	+0.006 [b]	
$[(Co^{II}OH_2)_2Fe^{III}{}_2]$	−0.090 [b]		$[(Fe^{III}OH_2)_2Co^{II}{}_2]$	−0.090	−0.200
$[(Mn^{II}OH_2)_2Fe^{III}{}_2]$	−0.080	−0.200	$[(Fe^{III}OH_2)_2Mn^{II}{}_2]$	−0.080	−0.200
$[(Mn^{III}OH_2)_2Fe^{III}{}_2]$ [c]	–	–	$[(Fe^{III}OH_2)_2Mn^{III}{}_2]$	−0.100	−0.200
$[(Cr^{III}OH_2)_2Fe^{III}{}_2]$ [c]	–	–	$[(Fe^{III}OH_2)_2Cr^{III}{}_2]$	−0.100	−0.330

[a] The two single-electron steps corresponding to the reduction of the Fe^{III} into Fe^{II} centres merge into a single wave which appears as a shoulder on the following wave that concerns the reduction of the Cu^{II} centres (Figure SI-2).
[b] The two single-electron steps corresponding to the reduction of the two Fe^{III} centres merge into a single two-electron wave.
[c] We have not succeeded in isolating these two compounds so far.

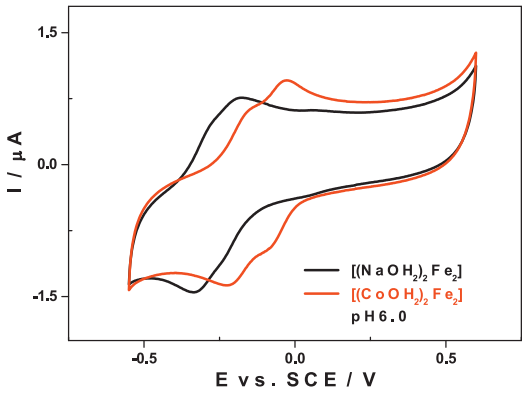

Fig. 2. Comparison of the CVs obtained with $[(NaOH_2)_2Fe_2(As_2W_{15}O_{56})_2]^{16-}$ (black) and with $[(CoOH_2)_2Fe_2(As_2W_{15}O_{56})_2]^{14-}$ (red) in 1.0 M $LiCH_3COO + CH_3COOH$/pH 6.0. The potential range is restricted to the Fe^{III} centres. POM concentration: 0.2 mM; working electrode: glassy carbon; reference electrode: SCE; auxiliary electrode: platinum; scan rate: 10 mV s^{-1}.

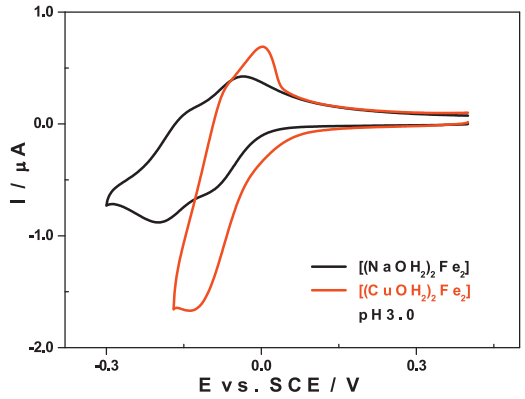

Fig. 3. Comparison of the CVs of $[(NaOH_2)_2Fe_2(As_2W_{15}O_{56})_2]^{16-}$ (black) and $[(CuOH_2)_2Fe_2(As_2W_{15}O_{56})_2]^{14-}$ (red) in 0.5 M $Li_2SO_4 + H_2SO_4$/pH 3.0. The potential range is restricted to the Fe^{III} centres. POM concentration: 0.2 mM; working electrode: glassy carbon; reference electrode: SCE; auxiliary electrode: platinum; scan rate: 10 mV s^{-1}.

two metallic centres M (with M = Cr^{III}, Mn^{II}, Mn^{III}, Co^{II}, Ni^{II}, Cu^{II} or Zn^{II}) and a new metallic cluster is obtained, $[(MOH_2)_2Fe^{III}{}_2]$; 2) the original structure corresponds to $[(NaOH_2)_2M_2(As_2W_{15}O_{56})_2]^{n-}$ characterised by the central metal cluster $[(NaOH_2)_2M_2]$ in which the Fe^{III} centres will take the place of the two sodium ions and will be found in an external position. Each Fe^{III} centre is bound to five oxygen atoms of the oxo-tungstic scaffold, the sixth position being occupied by a water molecule. In short, the two situations allow to study the behaviour of Fe^{III} centres found in two different coordination spheres, located either internally or externally, and in an environment influenced by the electronic configuration of the neighbouring metallic centre, either a sodium ion or a metal cation M (with M = Cr^{III}, Mn^{II}, Mn^{III}, Co^{II}, Ni^{II}, Cu^{II} or Zn^{II}).

In the first case, when two sodium ions are replaced by two d-type metal cations, the global negative charge decreases from −16 to −14, and the Fe^{III} centre reduction becomes easier (Fig. 2). For example, at pH 6, when going from $[(NaOH_2)_2Fe^{III}{}_2]$ to $[(Co^{II}OH_2)_2Fe^{III}{}_2]$, a maximum anodic shift of 0.130 V is observed for this family of compounds. In the case of $[(Ni^{II}OH_2)_2Fe^{III}{}_2]$, a species iso-electronic of the previous one, the shift is just of 0.020 V. If we consider the series of compounds substituted by divalent d-type cations, the cathodic peak potentials for the reduction of the Fe^{III} centres, $E_{pc}(Fe_1)$, follow the order: $E_{pc}(Fe_1)_{Ni} < E_{pc}(Fe_1)_{Mn} < E_{pc}(Fe_1)_{Zn} < E_{pc}(Fe_1)_{Cu} < E_{pc}(Fe_1)_{Co}$. Since all these species have the same global charge, parameters other than the charge have to be taken into account in order to explain the observed behaviour. All the divalent cations considered above have rather different electronic configurations as far as their valence d layers are concerned, as well as different acid/base properties in aqueous solution. The vicinity of metal centres M having differently filled d orbitals will directly influence the electronic density of the Fe^{III} centres and therefore their tendency to accept supplementary electrons.

However, this hypothesis, which is corroborated by theoretical calculation results (*vide infra*) does not always matches the experimental observations. When our experimental conditions are taken into account, we cannot base our reasoning exclusively on the electron distribution over the valence orbitals and ignore the interactions between species in solution. These interactions are dominated by proton exchange and therefore modulated by the pH of the medium and the acid/base properties of the compounds.

The influence on $E_{pc}(Fe_1)$ observed in 0.5 M $Li_2SO_4 + H_2SO_4$/pH 3.0, where the protonation effect cannot be ignored, is very different when compared to the one previously reported for pH 6. By and large, when the pH decreases from 6 to 3, the reduction peak potentials $E_{pc}(Fe_1)$ are anodically shifted, meaning that at a higher H^+ concentration (pH 3), electron transfer becomes easier. In fact, the Fe^{III} centre reduction in the present species is concomitant to protonation. The influence of the acid/base properties of the different complexes becomes predominant in this medium, and the most basic species will more easily and rapidly accept an extra electron. $[(Ni^{II}OH_2)_2Fe^{III}{}_2]$ becomes the cluster which is the easiest to reduce. $[(Co^{II}OH_2)_2Fe^{III}{}_2]$, which seems to be more difficult to reduce, $E_{pc}(Fe_1) = -0.090$ V, takes up two electrons in a single step. The behaviour of $[(Cu^{II}OH_2)_2Fe^{III}{}_2]$ is more peculiar, its cathodic peak potential at −0.130 V corresponding to the simultaneous reduction of the Fe^{III} and the Cu^{II} centres. CV and CPC have proven that three electrons are exchanged at the level of this wave without Cu^0 deposition (Fig. 3).

All in all, the protonation influence is too strong at pH 3 and does not allow a neat comparison between the Fe^{III} reduction potential as a function of the associated metal centre M within the cluster $[(MOH_2)_2Fe^{III}{}_2]$.

Let us consider again the medium 1.0 M $LiCH_3COO + CH_3COOH$/pH 6.0 in which the protonation influence is very limited, and compare the reduction potentials of the Fe^{III} centres internally located, $[(MOH_2)_2Fe^{III}{}_2]$, with those corresponding to the Fe^{III} centres externally located, $[(Fe^{III}OH_2)_2M_2]$. The observed trend in the reduction peak potentials, $E_{pc}(Fe_1)$, matches the theoretical calculation predictions in just two single cases: 1) when Cu^{II} centres are associated with the Fe^{III} centres, the first electron is exchanged at the same potential value (see Table 1) and is taken up by the Fe^{III} centres, irrespective of their relative positions, either externally or internally located; 2) the presence of Ni^{II} centres, which are not electroactive in the potential range used in the present work, strongly influences the electrochemical behaviour of the Fe^{III} centres found in the same STP. In fact, externally-located Fe^{III} centres are much easier to reduce than internally-located ones, both at pH 6 and at pH 3. The influence of the Fe^{III} centres location within the STP on their reduction peak potential values is more pronounced at pH 6 ($\{(E_{pc}(Fe_{ext}) - E_{pc}(Fe_{int})\}_{pH6} = 0.200$ V and $\{(E_{pc}(Fe_{ext}) - E_{pc}(Fe_{int})\}_{pH3} = 0.066$ V), a medium in which the protonation effect is limited and cannot account for the observed results on its own. Neither do electronic properties suffice to explain this behaviour. However, and as will be shown below, this is the natural and expected trend in STPs.

For the other metal centres M studied (Mn^{II}, Co^{II} and Zn^{II}), the experimental results disagree with the theoretical calculations, which foresee that externally-located Fe^{III} should be easier to reduce than internally-located ones. For example, when Zn^{II} and Fe^{III} centres are associated in the same STP, an inversion of the predicted trend is observed at pH 6, with internally-located

Table 2
Computed energy differences between the $[(MOH_2)_2Fe_2]$ and $[(FeOH_2)_2M_2]$ isomers (ΔE^{ox} and ΔE^{red}), 1e-reduction energies (REs) and their difference (ΔRE) for X = As compounds.[a].

	Initial charge	ΔE^{ox}	ΔE^{red}	RE	ΔRE[b]
$[(FeOH_2)_2Zn_2]$	14–	–0.508	–0.191	–4.233	0.316
$[(ZnOH_2)_2Fe_2]$	14–			–3.917	
$[(FeOH_2)_2Cu_2]$	14–	–0.576	–0.604	–4.127	–0.027
$[(CuOH_2)_2Fe_2]$	14–			–4.155	
$[(FeOH_2)_2Ni_2]$	14–	–0.395	–0.243	–4.196	0.152
$[(NiOH_2)_2Fe_2]$	14–			–4.044	
$[(FeOH_2)_2Co_2]$[c]	14–	–0.349	–0.260	–4.217[c]	0.325
$[(CoOH_2)_2Fe_2]$[c]	14–			–3.893[c]	
$[(FeOH_2)_2Mn_2]$	14–	–0.603	–0.330	–4.251	0.273
$[(MnOH_2)_2Fe_2]$	14–			–3.977	
$[(FeOH_2)_2Mn^{III}_2]$	12–	–1.03	–0.475	–4.777	0.553
$[(Mn^{III}OH_2)_2Fe_2]$	12–			–4.225	
$[(FeOH_2)_2Cr^{III}_2]$	12–	+0.303	+0.637	–4.517	0.334
$[(Cr^{III}OH_2)_2Fe_2]$	12–			–4.183	

[a] All values in eV.
[b] $\Delta RE = RE\{[(MOH_2)_2Fe_2]\} - RE\{[(FeOH_2)_2M_2]\}$, in eV.
[c] Values computed for X = P derivatives.

Fe^{III} centres being easier to reduce than externally-located ones ($\{(E_{pc}(Fe_{ext}) - E_{pc}(Fe_{int})\}_{pH6} = 0.030$ V). As far as the Mn^{II} and the Co^{II} centres are concerned, when associated with Fe^{III} centres in STPs, the reduction potentials of the latter are one and the same for both locations, a fact observed both at pH 6 and at pH 3. Last but not least, the study of STPs possessing both Fe^{III} and Zn^{II} centres at pH 3, a medium where protonation is important, revealed that the reduction of externally-located Fe^{III} centres is favoured, since their protonation is more accessible.

3.2. DFT calculations

Complementing the electrochemical measurements, DFT calculations have been carried out on the title compounds. This computational approach has proven successful in the study of most properties of POMs, and particularly redox processes. [75] We computed total molecular energies for the oxidised and 1e-reduced molecules to obtain the relative stabilities of each pair of isomers and the 1e REs, listed in Table 2.

The relative stability of the two positional isomers show, with the sole exception of $M = Cr^{III}$, and not considering protonation, that the DFT-optimised structures with internal Fe^{III} are more stable. For Zn^{II}, Cu^{II}, Ni^{II}, Co^{II} and Mn^{II} the energy difference between both oxidised isomers is $\Delta E^{ox} = 12$ kcal mol^{-1} on average, decreasing to $\Delta E^{red} = 7$–8 kcal mol^{-1} for the monoreduced species (X = P or As). Of course, the second reduction makes both isomeric forms even closer in energy. For Mn^{III}, $\Delta E^{ox} = 24$ kcal mol^{-1}, notably larger than for M = Co or Zn. We can thus consider that, in general, $M_2Fe^{III}_2$ is the dominant and most stable species in the oxidised form from a thermodynamic point of view. The fact that $\Delta E^{ox} > \Delta E^{red}$ is the computational proof that the $[(Fe^{III}OH_2)_2M_2]$ form is naturally more oxidant (more exothermic REs) than $[(MOH_2)_2Fe^{III}_2]$, not considering protonation effects. We will see below that the case of M = Ni is the expected one from calculations and not an exception within the family of studied systems.

In line with electrochemical measurements, DFT data reproduce the cathodic shift of 5–20 meV observed when As is replaced by P, a proof of quality of the computations. Also, among the studied structures, those with higher negative charge present less negative reduction energies, as shown in Table 2 (X = As). The range of reduction energies for the 14–charged species is –3.89 to –4.25 eV. For the 12–charged species, the values are comprised between –4.18 and –4.78 eV, that is, 0.3 to 0.5 eV more negative. These are quite exothermic though common values in POMs despite dealing with highly negatively charged molecules. [75] The reader must take into consideration that, if protonation was accounted for in the calculations, these reduction energies would be even more negative due to the concomitant decrease in the initial negative molecular charge.

The two rightmost columns of Table 2 list the REs for each system, and the difference between pairs of isomers (ΔRE), respectively, showing that the most exothermic (favourable) REs always correspond to $[(Fe^{III}OH_2)_2M_2]$ isomers, thus they are more oxidising than $[(MOH_2)_2Fe^{III}_2]$. The ΔRE differences for each M are not easy to rationalise although they all oscillate around a mean value of 0.3 eV. We discussed in the experimental section that the case with M = Ni presented a somewhat exceptional behaviour, even though it is clear from the computational data that all the systems except M = Cu behave the same way: without protonation, the systems with external Fe atoms are stronger oxidants.

A possible competition for the incoming electron(s) depends on the nature and position of the metal atoms in the equatorial region. How is the incoming electron shared within the equatorial cluster? To know where the electron is located from calculations, the oxidation state of the relevant metal atoms has to be monitored by analysing their atomic spin populations (ASPs, Table 3) before and after adding one electron to the molecule. These ASPs have a direct correspondence with the number of excess (α–β) electrons in the valence d shell of metal atoms shown in Fig. 4. Since we deal with M^{n+} ions in a pseudo-octahedral ligand field, their valence d orbitals ideally split into the two sets represented, accommodating 3 (Cr^{III}) to 10 (Zn^{II}) electrons. We consider that each metal atom is in its high spin configuration owing to the weak ligand field exerted by the oxo groups and the terminal water ligand. Consequently, only d^3 (Cr^{III})- and d^4 (Mn^{III})-based compounds are allowed to accept a new spin-up electron. However, if Fe^{III} (a d^5 atom cation) accepts

Table 3
Atomic spin populations (ASPs) for the equatorial metal atoms[a] in the oxidised and reduced forms.

		External Fe				Internal Fe	
		Oxidised	Reduced			Oxidised	Reduced
$[(FeOH_2)_2Zn_2]$	Zn	0.001	−0.005	$[(ZnOH_2)_2Fe_2]$	Fe	4.122	3.986
	Fe	4.127	3.999		Zn	−0.005	−0.006
$[(FeOH_2)_2Cu_2]$	Cu	0.700	0.678	$[(CuOH_2)_2Fe_2]$	Fe	4.137	4.044
	Fe	4.129	4.009		Cu	0.652	0.570
$[(FeOH_2)_2Ni_2]$	Ni	1.704	1.699	$[(NiOH_2)_2Fe_2]$	Fe	4.126	3.996
	Fe	4.137	4.005		Ni	1.699	1.695
$[(FeOH_2)_2Co_2]$	Co	2.714	2.744	$[(CoOH_2)_2Fe_2]$	Fe	4.127	3.992
	Fe	4.122	3.994		Co	2.719	2.715
$[(FeOH_2)_2Mn_2]$	Mn	4.786	4.783	$[(MnOH_2)_2Fe_2]$	Fe	4.114	3.974
	Fe	4.110	3.985		Mn	4.807	4.805
$[(FeOH_2)_2Mn^{III}{}_2]$	Mn	3.760	4.365	$[(Mn^{III}OH_2)_2Fe_2]$	Fe	4.119	4.115
	Fe	4.106	4.107		Mn	3.901	4.378
$[(FeOH_2)_2Cr^{III}{}_2]$	Cr	2.941	2.938	$[(Cr^{III}OH_2)_2Fe_2]$	Fe	4.110	3.978
	Fe	4.138	4.007		Cr	2.982	2.969

[a] The initial oxidation state of Fe is +III, and unless otherwise indicated, that of the other elements is +II.

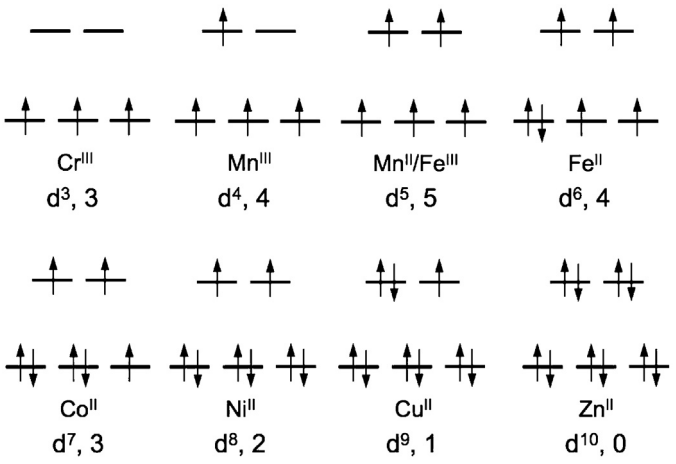

Fig. 4. Electronic configurations deriving from a weak octahedral field for first row transition metals. The number of α–β electrons is shown.

an electron, it will enter as spin-down to give the d^6 configuration, thus cancelling out part of the initial spin-up density.

In the computed 1e reductions it must be considered that the extra electron formally splits between, at least, two metal centres by reasons of molecular symmetry. In addition to this, electron polarisation to the neighbouring oxygens make the ASPs variations small from the oxidised to the reduced states as can be observed in the ASPs of metal ions listed in Table 3 (note that the values are smaller than the *formal* ones) except for $M = Mn^{III}$, no matter if Fe^{III} is in the internal or the external position. This is an important observation since it helps to understand that the process taking place is $Fe^{III} + e \rightarrow Fe^{II}$ in all cases but for $M = Mn^{III}$.

The molecular orbital representation in Fig. 5 proves that the molecular orbital accepting the extra electron during the reduction process belongs to the Fe atoms in both isomers, as illustrated in the data presented above. Following the 'general' trend obtained by DFT calculations for M^{II}-Fe^{III} mixtures, Fe^{III} centres are reduced irrespective of the position they occupy in the equatorial cluster. The higher oxidation state of Fe^{III} compared with its M^{II} partners is determinant to this issue: no M^{II} ion from the first period of transition metals will achieve the M^{I} state before Fe^{III} is reduced to Fe^{II}.

Although it could not be fully characterised by electrochemistry, DFT calculations reveal that both isomers of the Mn^{III}–containing STPs are firstly reduced in the Mn^{III} centres to reach the Mn^{II} state. This is shown in Table 3 by an increase of the net spin density on the high spin Mn atoms, indicating that the $Mn^{III} \rightarrow Mn^{II}$ process takes place. It is expected that Mn^{III} reduces before Fe^{III} owing to the more favourable $d^4 \rightarrow d^5$ process when compared to $d^5 \rightarrow d^6$. The structure with internal Mn^{III} atoms is more easily reduced by 0.55 eV. After both Mn^{III} atoms are reduced, Fe^{III} atoms gain electrons. Fig. 6 shows a scheme of the molecular orbitals involved in the reduction processes when entering a spin-up or a spin-down electron.

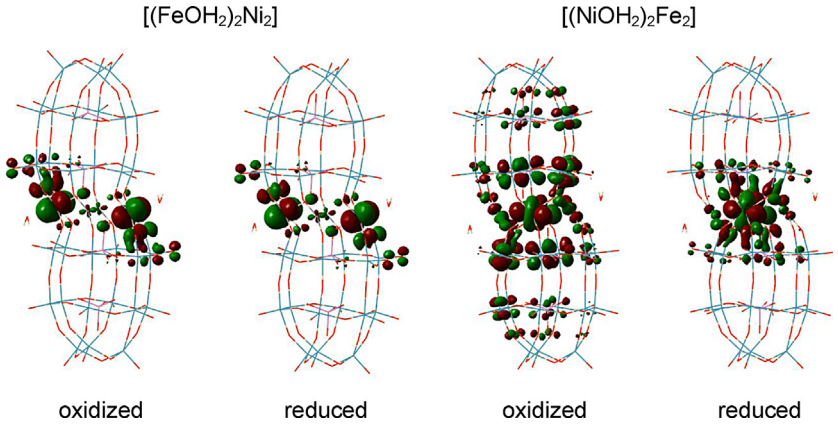

Fig. 5. Fe-like molecular orbitals of $[(FeOH_2)_2Ni_2]$, with external-Fe atoms, and $[(NiOH_2)_2Fe_2]$, with internal-Fe atoms, before (oxidised) and after (reduced) accepting the extra electron.

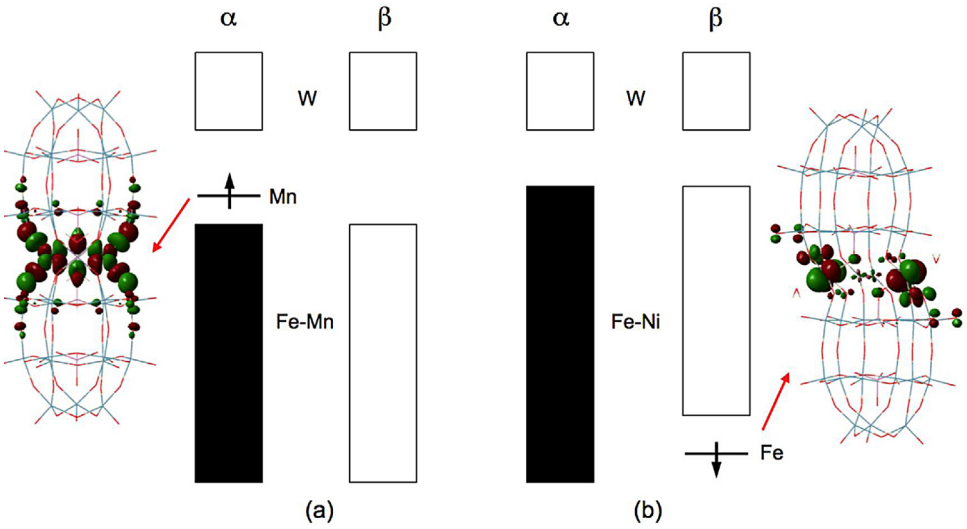

Fig. 6. Two examples of single-electron reduction with the incoming electron (arrow) having either (a) an α spin —case of $Fe_2Mn^{III}{}_2$— or (b) a β spin —case of Fe_2Ni_2 and others. Black and white blocks represent filled and empty metal-like molecular orbitals, respectively.

All in all, the Fe-Cu case is the one presenting the most exceptional behaviour within the group of divalent M atoms since both isomers are reduced at very similar energies (only 27 and 18 meV for the RE difference for X = As and P, respectively). Interestingly, the $[Cu(OH_2)_2Fe_2]$ isomer is largely more stable than its external-Fe counterpart by –0.576 eV, in line with the other members of the family. Its specific quality is that an incoming electron cannot distinguish between the two isomers and 'sees' them as equally oxidising, so the isomerism is electrochemically irrelevant. As a proof of concept, Table 3 shows a net decrease in ASPs for both Fe and Cu atoms when going from the oxidised to the reduced form, more clearly for the $[(CuOH_2)_2Fe_2]$ isomer. The incoming electron is *shared* between the four equatorial metal atoms, indicating an equal electronegativity in Cu^{II} and Fe^{III} and explaining the experimental and theoretical redox behaviour of this pair of isomers.

4. Conclusions

We have carried out an innovative study on the electrochemical behaviour of mixed d metal-iron containing Wells-Dawson sandwich-type complexes $[(FeOH_2)_2M_2(X_2W_{15}O_{56})_2]^{14-}$ and $[(MOH_2)_2Fe_2(X_2W_{15}O_{56})_2]^{14-}$ (with $M = Cr^{III}$, Mn^{II}, Mn^{III}, Co^{II}, Ni^{II}, Cu^{II} or Zn^{II} and $X = P^V$ or As^V). This study combined experimental methods (cyclic voltammetry and controlled potential coulometry) with theoretical calculations and allowed us to determine redox potential values associated with the reduction of the Fe^{III} centres in these species. In most of the cases, the reduction of the two Fe^{III} centres takes place in two successive single-electron steps, each electron being delocalised over the two centres. DFT calculation methods led to a compilation of molecular energies associated with the one-electron oxidised and reduced forms of all the compounds in the family. It seems that the most stable isomers are those where Fe^{III} centres are internally-located, $[(MOH_2)_2Fe_2]$. Consequently, their reduction is more difficult than those having externally-located Fe^{III} isomers, [60] $[(FeOH_2)_2M_2]$. Some experimental results revealed a few exceptions to this rule which have not been rationalised yet. In summary, in the majority of the cases studied, we were able to rationalise the redox behaviour and the electron distribution within the valence shell orbitals of these compounds, which opens the way to improved prediction capabilities of their electrochemical and magnetic properties.

Acknowledgements

This work was supported by the Centre National de la Recherche Scientifique (UMR 8180, UMR 8000), the University of Versailles, the University Paris-Sud, the Spanish Ministry of Science and Innovation (MICINN) (project N° CTQ2011-29054-C02-01/BQU) and the DGR of the Generalitat de Catalunya (grant N° 2009SGR462 and the XRQTC). X.L. thanks the Ramón y Cajal program (grant number RYC-2008-02493). This collaboration takes place in the context of the COST PoCheMoN action supported by the European Research Area.

Appendix A. Supplementary data

Supplementary data associated with this article can be found, in the online version, at http://dx.doi.org/10.1016/j.electacta.2014.01.151.

References

[1] M.T. Pope, Heteropoly and Isopoly Oxometalates, Springer-Verlag, Berlin, 1983.
[2] R. Contant, G. Hervé, The heteropolyoxotungstates: Relationships between routes of formation and structures, Reviews in Inorganic Chemistry 22 (2002) 63–111.
[3] D.-L. Long, R. Tsunashima, L. Cronin, Polyoxometalates, Building Blocks for Functional Nanoscale Systems, Angewandte, Chemie International Edition 49 (2010) 1736–1758.
[4] T.J.R. Weakley, H.T. Evans Jr., J.S. Showell, G.F. Tourné, C.M. Tourné, 18-Tungstotetracobalto(II)diphosphate and related anions: a novel structural class of heteropolyanions, Journal of the Chemical Society, Chemical Communications 4 (1973) 139–140.
[5] R.G. Finke, M. Droege, J.R. Hutchinson, O. Gansow, Trivacant heteropolytungstate derivatives: the rational synthesis, characterization, and tungsten-183 NMR spectra of $P_2W_{18}M_4(H_2O)_2O_{68}{}^{10-}$ (M = cobalt, copper, zinc), Journal of the American Chemical Society 103 (1981) 1587–1589.
[6] R.G. Finke, M.W. Droege, Trivacant heteropolytungstate derivatives. 2. Synthesis, characterization, and tungsten-183 NMR of $P_4W_{30}M_4(H_2O)_2O_{112}{}^{16-}$ (M = Co, Cu, Zn), Inorganic Chemistry 22 (1983) 1006–1008.
[7] H.T. Evans, C.M. Tourné, G.F. Tourné, T.J.R. Weakley, *X*-Ray crystallographic and tungsten-183 nuclear magnetic resonance structural studies of the $[M_4(H_2O)_2(XW_9O_{34})_2]^{10-}$ heteropolyanions (M = CO^{II} or Zn, X = P or As), Journal of the Chemical Society, Dalton Transastions 12 (1986) 2699–2705.
[8] S.H. Wasfi, A.L. Rheingold, G.F. Kokoszka, A.S. Goldstein, Preparation, structure, and magnetic properties of $Na_{10}Fe_4Cu_2W_{18}O_{70}H_6.29H_2O$, containing the double Keggin anion $[Fe_4Cu_2W_{18}O_{70}H_6]^{10-}$, Inorganic Chemistry 26 (1987) 2934–2939.
[9] R.G. Finke, M.W. Droege, P.J. Domaille, Trivacant heteropolytungstate derivatives. 3. Rational syntheses, characterization, two-dimensional tungsten-183 NMR, and properties of tungstometallophosphates $P_2W_{18}M_4(H_2O)_2O_{68}{}^{10-}$ and

$P_4W_{30}M_4(H_2O)_2O_{112}^{16-}$ (M = cobalt, copper, zinc), Inorganic Chemistry 26 (1987) 3886–3896.
[10] C.M. Tourné, G.F. Tourné, F. Zonnevijlle, Chiral polytungstometalates $[WM_3(H_2O)_2(XW_9O_{34})_2]^{12-}$ (X = M = Zn or Co^{II}) and their M-substituted derivatives. Syntheses, chemical, structural and spectroscopic study of some D,L sodium and potassium salts, Journal of the Chemical Society, Dalton Transactions 1 (1991) 143–155.
[11] N. Casañ-Pastor, J. Bas-Serra, E. Coronado, G. Pourroy, L.C.W. Baker, First ferromagnetic interaction in a heteropoly complex: $[Co^{II}_4O_{14}(H_2O)_2(PW_9O_{27})_2]^{10-}$. Experiment and theory for intramolecular anisotropic exchange involving the four Co(II) atoms, Journal of the American Chemical Society 114 (1992) 10380–10383.
[12] C.J. Gómez-García, E. Coronado, P. Gómez-Romero, N. Casañ-Pastor, Crystal structure and magnetic properties of $K_{5.5}Na_{1.5}[PW_{10}Cu_2(H_2O)_2O_{38}].13H_2O$. Substituted Keggin heteropolytungstates of the type $PW_{10}Cu_2$ containing exchange-coupled copper pairs, Inorganic Chemistry 32 (1993) 89–93.
[13] C.J. Gómez-García, E. Coronado, P. Gómez-Romero, N. Casañ-Pastor, A tetranuclear rhomblike cluster of manganese(II). Crystal structure and magnetic properties of the heteropoly complex $K_{10}[Mn_4(H_2O)_2(PW_9O_{34})_2].20H_2O$, Inorganic Chemistry 32 (1993) 3378–3381.
[14] J.M. Clemente-Juan, E. Coronado, J.R. Galán-Mascarós, C.J. Gómez-García, Increasing the Nuclearity of Magnetic Polyoxometalates. Syntheses, Structures, and Magnetic Properties of Salts of the Heteropoly Complexes $[Ni_3(H_2O)_3(PW_{10}O_{39})H_2O]^{7-}$, $[Ni_4(H_2O)_2(PW_9O_{34})_2]^{10-}$, and $[Ni_9(OH)_3(H_2O)_6(HPO_4)_2(PW_9O_{34})_3]^{16-}$, Inorganic Chemistry 38 (1999) 55–63.
[15] X.-Y. Zhang, C.J. O'Connor, G.B. Jameson, M.T. Pope, High-Valent Manganese in Polyoxotungstates. 3. Dimanganese Complexes of gamma-Keggin Anions, Inorganic Chemistry 35 (1996) 30–34.
[16] T.J.R. Weakley, R.G. Finke, Single-crystal x-ray structures of the polyoxotungstate salts $K_{8.3}Na_{1.7}[Cu_4(H_2O)_2(PW_9O_{34})_2].24H_2O$ and $Na_{14}Cu[Cu_4(H_2O)_2(P_2W_{15}O_{56})_2].53H_2O$, Inorganic Chemistry 29 (1990) 1235–1241.
[17] A.M. Khenkin, C.L. Hill, Selective Homogeneous Catalytic Epoxidation of Alkenes by Hydrogen Peroxide Catalysed by Oxidatively- and Solvolytically-resistant Polyoxometalate Complexes, Mendeleev Commun. 3 (1993) 140–141.
[18] C.J. Gómez-García, J.J. Borrás-Almenar, E. Coronado, L. Ouahab, Single-Crystal X-ray Structure and Magnetic Properties of the Polyoxotungstate Complexes $Na_{16}[M_4(H_2O)_2(P_2W_{15}O_{56})_2].nH_2O$ (M = Mn^{II}, n = 53; M = Ni^{II}, n = 52): An Antiferromagnetic Mn^{II} Tetramer and a Ferromagnetic Ni^{II} Tetramer, Inorganic Chemistry 33 (1994) 4016–4022.
[19] R.G. Finke, T.J.R. Weakley, Structure of sodium bis(pentadecatungstodiphosphato)diaquatetrazincate hydrate (16:1:50), Journal of Chemical. Crystallography 24 (1994) 123–128.
[20] X. Zhang, Q. Chen, D.C. Duncan, C. Campana, C.L. Hill, Multiiron Polyoxoanions. Syntheses, Characterization, X-ray Crystal Structures, and Catalysis of H_2O_2-Based Hydrocarbon Oxidations by $[Fe^{III}_4(H_2O)_2(P_2W_{15}O_{56})_2]^{12-}$, Inorganic Chemistry 36 (1997) 4208–4215.
[21] X. Zhang, Q. Chen, D.C. Duncan, R.J. Lachicotte, C.L. Hill, Multiiron Polyoxoanions. Synthesis, Characterization, X-ray Crystal Structure, and Catalytic H_2O_2-Based Alkene Oxidation by $[(n\text{-}C_4H_9)_4N]_6[Fe^{III}_4(H_2O)_2(PW_9O_{34})_2]$, Inorganic Chemistry 36 (1997) 4381–4386.
[22] M. Rusu, G. Marcu, D. Rusu, C. Rosu, A.-R. Tomsa, Uranium(IV) polyoxotungstophosphates, Journal of Radioanalytical and Nuclear Chemistry 242 (1999) 467–472.
[23] L.H. Bi, E.-B. Wang, J. Peng, R.D. Huang, L. Xu, C.W. Hu, Crystal Structure and Replacement Reaction of Coordinated Water Molecules of the Heteropoly Compounds of Sandwich-Type Tungstoarsenates, Inorganic Chemistry 39 (2000) 671–679.
[24] L.H. Bi, R.D. Huang, J. Peng, E.-B. Wang, Y.-H. Wang, C.-W. Hu, Rational syntheses, characterization, crystal structure, and replacement reactions of coordinated water molecules of $[As_2W_{18}M_4(H_2O)_2O_{68}]^{10-}$ (M = Cd, Co, Cu, Fe, Mn, Ni or Zn), Journal of the Chemical Society, Dalton Transactions 2 (2001) 121–129.
[25] U. Kortz, S. Isber, M.H. Dickman, D. Ravot, Sandwich-Type Silicotungstates: Structure and Magnetic Properties of the Dimeric Polyoxoanions $[\{SiM_2W_9O_{34}(H_2O)\}_2]^{12-}$ (M = Mn^{2+}, Cu^{2+}, Zn^{2+}), Inorganic Chemistry 39 (2000) 2915–2922.
[26] X. Zhang, T.M. Anderson, Q. Chen, C.L. Hill, A Baker - Figgis Isomer of Conventional Sandwich Polyoxometalates. $H_2Na_{14}[Fe^{III}_2(NaOH_2)_2(P_2W_{15}O_{56})_2]$, a Diiron Catalyst for Catalytic H_2O_2-Based Epoxidation, Inorganic Chemistry 40 (2001) 418–419.
[27] T.M. Anderson, K.I. Hardcastle, N. Okun, C.L. Hill, Asymmetric Sandwich-Type Polyoxoanions. Synthesis, Characterization, and X-ray Crystal Structures of Diferric Complexes $[TM^{II}Fe^{III}_2(P_2W_{15}O_{56})(P_2TM^{II}_2W_{13}O_{52})]^{16-}$, TM = Cu or Co, Inorganic Chemistry 40 (2001) 6418–6425.
[28] X. Zhang, C.L. Hill, Multi-iron polyoxoanions. Synthesis, characterization and catalysis of H_2O_2-based hydrocarbon oxidations, Chemical Industries 75 (1998) 519–524.
[29] L. Ruhlmann, L. Nadjo, J. Canny, R. Contant, R. Thouvenot, Di- and Tetranuclear Dawson-Derived Sandwich Complexes: Synthesis, Spectroscopic Characterization, and Electrochemical Behavior, European Journal of Inorganic Chemistry 4 (2002) 975–986.
[30] L. Ruhlmann, J. Canny, R. Contant, R. Thouvenot, Di- and Tricobalt Dawson Sandwich Complexes: Synthesis, Spectroscopic Characterization, and Electrochemical Behavior of $Na_{18}[(NaOH_2)_2Co_2(P_2W_{15}O_{56})_2]$ and $Na_{17}[(NaOH_2)Co_3(H_2O)(P_2W_{15}O_{56})_2]$, Inorganic Chemistry 41 (2002) 3811–3819.
[31] T.M. Anderson, X. Zhang, K.I. Hardcastle, C.L. Hill, Reactions of Trivacant Wells - Dawson Heteropolytungstates. Ionic Strength and Jahn - Teller Effects on Formation in Multi-Iron Complexes, Inorganic Chemistry 41 (2002) 2477–2488.
[32] U. Kortz, M.G. Savelieff, B.M. Bassil, B. Keita, L. Nadjo, Synthesis and Characterization of Iron(III)-Substituted, Dimeric Polyoxotungstates, $[Fe_4(H_2O)_{10}(\beta\text{-}XW_9O_{33})_2]^{n-}$ ($n = 6$, X = As^{III}, Sb^{III}; $n = 4$, X = Se^{IV}, Te^{IV}), Inorganic Chemistry 41 (2002) 783–789.
[33] I.M. Mbomekalle, B. Keita, L. Nadjo, P. Berthet, W.A. Neiwert, C.L. Hill, M.D. Ritorto, T.M. Anderson, Manganous heteropolytungstates. Synthesis and heteroatom effects in Wells–Dawson-derived sandwich complexes, Dalton Transactions 13 (2003) 2646–2650.
[34] I.M. Mbomekalle, B. Keita, L. Nadjo, P. Berthet, K.I. Hardcastle, C.L. Hill, T.M. Anderson, Multi-Iron Tungstodiarsenates. Synthesis, Characterization, and Electrocatalytic Studies of $\alpha\beta\beta\alpha$-$(Fe^{III}OH_2)_2Fe^{III}_2(As_2W_{15}O_{56})_2^{12-}$, Inorganic Chemistry 42 (2003) 1163–1169.
[35] I.M. Mbomekalle, B. Keita, L. Nadjo, W.A. Neiwert, L. Zhang, K.I. Hardcastle, C.L. Hill, T.M. Anderson, Lacunary Wells - Dawson Sandwich Complexes - Synthesis, Characterization, and Stability Studies of Multi-Iron Species, European Journal of Inorganic Chemistry 21 (2003) 3924–3928.
[36] L. Ruhlmann, J. Canny, J. Vaissermann, R. Thouvenot, Mixed-metal sandwich complexes $[M^{II}_2(H_2O)_2Fe^{III}_2(P_2W_{15}O_{56})_2]^{14-}$ (M^{II}=Co, Mn): Synthesis and stability. The molecular structure of $[M^{II}_2(H_2O)_2Fe^{III}_2(P_2W_{15}O_{56})_2]^{14-}$, Dalton Transactions (2004) 794–800.
[37] X. Fang, T.M. Anderson, C. Benelli, C.L. Hill, Polyoxometalate-Supported Y–and Yb^{III}–Hydroxo/Oxo Clusters from Carbonate-Assisted Hydrolysis, Chemistry A European Journal 11 (2005) 712–718.
[38] F. Hussain, M. Reicke, V. Janowski, S. de Silva, J. Futuwi, U. Kortz, Some indium(III)-substituted polyoxotungstates of the Keggin and Dawson types, Comptes Rendus de Chimie 8 (2005) 1045–1056.
[39] I.M. Mbomekalle, R. Cao, K.I. Hardcastle, C.L. Hill, M. Ammam, B. Keita, L. Nadjo, T.M. Anderson, Synthesis, structural characterization, and electrocatalytic studies of $\alpha\beta\beta\alpha$-$(Zn^{II}OH_2)_2(Fe^{III})_2(X_2W_{15}O_{56})_2^{14-}$ (X = P or As), Comptes Rendus de Chimie 8 (2005) 1077–1086.
[40] T.M. Anderson, X. Fang, I.M. Mbomekalle, B. Keita, L. Nadjo, K.I. Hardcastle, A. Farsidjani, C.L. Hill, Structural and Electrochemical Studies of Dicupric Sandwich-Type Complexes Journal of Cluster Science 17 (2006) 183–195.
[41] L. Ruhlmann, C. Costa-Coquelard, J. Canny, R. Thouvenot, Mixed-Metal Dawson Sandwich Complexes: Synthesis, Spectroscopic Characterization and Electrochemical Behaviour of $Na_{16}[M^{II}Co_3(H_2O)_2(P_2W_{15}O_{56})_2]$ (M = Mn, Co, Ni, Zn and Cd), European Journal of Inorganic Chemistry 11 (2007) 1493–1500.
[42] L. Ruhlmann, C. Costa-Coquelard, J. Canny, R. Thouvenot, Electrochemical and electrocatalytical investigations on the trimanganese sandwich complex $[NaMn_3(H_2O)_2(P_2W_{15}O_{56})_2]^{17-}$, Journal of Electroanalytical Chemistry 603 (2007) 260–268.
[43] C.P. Pradeep, D.-L. Long, P. Koegerler, L. Cronin, Controlled assembly and solution observation of a 2.6 nm polyoxometalate 'super' tetrahedron cluster: $[KFe_{12}(OH)_{18}(\alpha\text{-}1,2,3\text{-}P_2W_{15}O_{56})_4]^{29-}$, Chemical Communications 41 (2007) 4254–4256.
[44] B. Botar, P. Koegerler, Acetate-driven polyoxometalate demetalation: An open-shell diiron polytungstate comprising two rotational Keggin isomers, Dalton Transactions (2008) 3150–3152.
[45] C. Ritchie, A. Ferguson, H. Nojiri, H.N. Miras, Y.-F. Song, D.-L. Long, E. Burkholder, M. Murrie, P. Kogerler, E.K. Brechin, L. Cronin, Polyoxometalate-Mediated Self-Assembly of Single-Molecule Magnets: $\{[XW_9O_{34}]_2[Mn^{III}_4Mn^{II}_2O_4(H_2O)_4]\}^{12-}$, Angewandte Chemistry International Edition 47 (2008) 5609–5612.
[46] C. Lydon, C. Busche, N.M. Haralampos, A. Delf, D.-L. Long, L. Yellowlees, L. Cronin, Nanoscale Growth of Molecular Oxides: Assembly of a $\{V_6\}$ Double Cubane Between Two Lacunary $\{P_2W_{15}\}$ Polyoxometalates, Angewandte Chemie International Editional 51 (2012) 2115–2118.
[47] Z. Luo, P. Kögerler, R. Cao, C.L. Hill, Synthesis, Structure, and Magnetism of a Polyoxometalate with Coordinatively Unsaturated d-Electron-Transition Metal Centers, Inorganic Chemistry 48 (2009) 7812–7817.
[48] J.D. Compain, P. Mialane, A. Dolbecq, I.M. Mbomekallé, J. Marrot, F. Sécheresse, C. Duboc, E. Rivière, Structural, Magnetic, EPR, and Electrochemical Characterizations of a Spin-Frustrated Trinuclear Cr^{III} Polyoxometalate and Study of Its Reactivity with Lanthanum Cations, Inorganic Chemistry 49 (2010) 2851–2858.
[49] Y. Hou, L. Xu, M.J. Cichon, S. Lense, K.I. Hardcastle, C.L. Hill, A New Family of Sandwich-Type Polytungstophosphates Containing Two Types of Metals in the Central Belt: $M'_2M_2(PW_9O_{34})_2^{12-}$ (M′ = Na or Li, M = Mn^{2+}, Co^{2+}, Ni^{2+}, and Zn^{2+}), Inorganic Chemistry 49 (2010) 4125–4132.
[50] B. Botar, A. Ellern, P. Kögerler, Acetate-controlled demetalation in multiiron polyoxometalates: A triiron cluster trapped between β- and (-Keggin isomers, Dalton Transactions (2009) 5606–5608.
[51] T. Yamase, H. Abe, E. Ishikawa, H. Nojiri, Y. Ohshima, Structure and Magnetism of $[n\text{-}BuNH_3]_{12}[Cu_4(GeW_9O_{34})_2]\cdot 14H_2O$ Sandwiching a Rhomblike Cu_4^{8+} Tetragon through α-Keggin Linkage, Inorganic Chemistry 48 (2009) 138–148.
[52] C.L. Hill, Guest Editor, Polyoxometalates, Chemical Review 98 (1998) 1–389.
[53] B. Keita, L. Nadjo, Polyoxometalate-based homogeneous catalysis of electrode reactions: Recent achievements, J. Mol. Cat. A 262 (2007) 190–215.
[54] D. Long, -L., Burkholder E., Cronin, L., Polyoxometalate clusters, nanostructures and materials: From self-assembly to designer materials and devices, Chemical Society Review 36 (2007) 105–121.
[55] U. Kortz, A. Müller, J. Slageren, v.J. Schnack, N.S. Dalal, M. Dressel, Polyoxometalates: Fascinating Structures, Unique Magnetic Properties, Coordination Chemistry Review 253 (2009) 2315–2327.

[56] B. Keita, T. Liu, L. Nadjo, Synthesis of remarkably stabilized metal nanostructures using polyoxometalates, Journal of Material Chemistry 19 (2009) 19–33.
[57] Q. Yin, J.M. Tan, C. Besson, Y.V. Geletii, D.G. Musaev, A.E. Kuznetsov, Z. Luo, K.I. Hardcastle, C.L. Hill, A Fast Soluble Carbon-Free Molecular Water Oxidation Catalyst Based on Abundant Metals, Science 328 (2010) 342–345.
[58] J.J. Stracke, R.G. Finke, Electrocatalytic Water Oxidation Beginning with the Cobalt Polyoxometalate $[Co_4(H_2O)_2(PW_9O_{34})_2]^{10-}$: Identification of Heterogeneous CoO_x as the Dominant Catalyst, Journal of the American Chemistry Society 133 (2011) 14872–14875.
[59] X.Y. Zhang, G.B. Jameson, C.J. O'Connor, M.T. Pope, High-valent manganese in polyoxotungstates-II. Oxidation of the tetramanganese heteropolyanion $[Mn_4(H_2O)_2(PW_9O_{34})_2]^{10-}$, Polyhedron 15 (1996) 917–922.
[60] S. Romo, J.A. Fernández, J.M. Maestre, B. Keita, L. Nadjo, C. de Graaf, J.M. Poblet, Density Functional Theory and ab Initio Study of Electronic and Electrochemistry Properties of the Tetranuclear Sandwich Complex $[Fe^{III}_4(H_2O)_2(PW_9O_{34})_2]^{6-}$, Inorganic Chemistry 46 (2007) 4022–4027, 46.
[61] J.M. Clemente-Juan, E. Coronado, A. Gaita-Arino, C. Gimenez-Saiz, H.-U. Gudel, A. Sieber, R. Bircher, H. Mutka, Magnetic Polyoxometalates: Anisotropic Exchange Interactions in the Co^{II}_3Moiety of $[(NaOH_2)Co_3(H_2O)(P_2W_{15}O_{56})_2]^{17-}$, Inorganic Chemistry 44 (2005) 3389–3395.
[62] S. Reinoso, J. Ramón Galán-Mascarós, Heterometallic 3d - 4f Polyoxometalate Derived from the Weakley-Type Dimeric Structure, Inorganic Chemistry 49 (2010) 377–379.
[63] S. Reinoso, J. Ramón Galán-Mascarós, L. Lezama, New Type of Heterometallic 3d–4f Rhomblike Core in Weakley-Like Polyoxometalates, Inorganic Chemistry 50 (2011) 9587–9593.
[64] I.M. Mbomekalle, P. Mialane, A. Dolbecq, J. Marrot, F. Sécheresse, P. Berthet, B. Keita, L. Nadjo, Rational Synthesis, Structure, Magnetism and Electrochemistry of Mixed Iron–Nickel-Containing Wells–Dawson-Fragment-Based Sandwich-Type Polyoxometalates, European Journal of Inorganic Chemistry 34 (2009) 5194–5204.
[65] M. Lebrini, I.M. Mbomekalle, A. Dolbecq, J. Marrot, P. Berthet, J. Ntienoue, F. Sécheresse, J. Vigneron, A. Etcheberry, Manganese(III)-Containing Wells–Dawson Sandwich-Type Polyoxometalates: Comparison with their Manganese(II) Counterparts, Inorganic Chemistry 50 (2011) 6437–6448.
[66] B. Keita, I.M. Mbomekallé, L. Nadjo, Redox behaviours and electrocatalytic properties of copper within Dawson structure-derived sandwich heteropolyanions $[Cu_4(H_2O)_2(X_2W_{15}O_{56})_2]^{16-}$ (X = P or As), Electrochemistry Communications 5 (2003) 830–837.
[67] I.M. Mbomekallé, B. Keita, L. Nadjo, R. Contant, B. Belai, M.T. Pope, Rationalization and improvement of the syntheses of two octadecatungstoarsenates: the novel α-$K_7[H_4AsW_{18}O_{62}]\cdot 18H_2O$ and the well-known symmetrical α-$K_6[As_2W_{18}O_{62}]\cdot 14H_2O$, Inorganica Chimica Acta 342 (2003) 219–228.
[68] R. Contant, R. Thouvenot, Hétéropolyanions de type Dawson. 2. Synthèses de polyoxotungstoarsénates lacunaires dérivant de l'octadécatungstodiarsénate. Étude structurale par RMN du tungstène-183 des octadéca(molybdotungstovanado)diarsénates apparentés, Canadian Journal of Chemistry 69 (1991) 1498–1506.
[69] N. Vila, P.A. Aparicio, F. Sécheresse, J.M. Poblet, X. López, I.M. Mbomekallé, Electrochemical Behavior of α_1/α_2-$[Fe(H_2O)P_2W_{17}O_{61}]^{7-}$Isomers in Solution: Experimental and DFT Studies, Inorganic Chemistry 51 (2012) 6129–6138.
[70] Frisch, M. J.; Trucks, G. W.; Schlegel, H. B.; Scuseria, G. E.; Robb, M. A.; Cheeseman, J. R.; Scalmani, G.; Barone, V.; Mennucci, B.; Petersson, G. A.; Nakatsuji, H. C., M.; Li, X.; Hratchian, H. P.; Izmaylov, A. F.; Bloino, J.; Zheng, G.; Sonnenberg, J. L.; Hada, M.; Ehara, M.; Toyota, K.; Fukuda, R.; Hasegawa, J.; Ishida, M.; Nakajima, T.; Honda, Y.; Kitao, O.; Nakai, H.; Vreven, T.; Montgomery, Jr., J. A.; Peralta, J. E.; Ogliaro, F.; Bearpark, M.; Heyd, J. J.; Brothers, E.; Kudin, K. N.; Staroverov, V. N.; Kobayashi, R.; Normand, J.; Raghavachari, K.; Rendell, A.; Burant, J. C.; Iyengar, S. S.; Tomasi, J.; Cossi, M.; Rega, N.; Millam, N. J.; Klene, M.; Knox, J. E.; Cross, J. B.; Bakken, V.; Adamo, C.; Jaramillo, J.; Gomperts, R.; Stratmann, R. E.; Yazyev, O.; Austin, A. J.; Cammi, R.; Pomelli, C.; Ochterski, J. W.; Martin, R. L.; Morokuma, K.; Zakrzewski, V. G.; Voth, G. A.; Salvador, P.; Dannenberg, J. J.; Dapprich, S.; Daniels, A. D.; Farkas, Ö.; Foresman, J. B.; Ortiz, J. V.; Cioslowski, J.; Fox, D. J., In Revision A.1; Gaussian, Inc.: Wallingford CT (2009).
[71] C.T. Lee, W.T. Yang, R.G. Parr, Development of the Colle-Salvetti correlation-energy formula into a functional of the electron density, Physical Review B 37 (1988) 785–789.
[72] P.J. Hay, W.R. Wadt, AB initio effective core potentials for molecular calculations - potentials for the transition-metal atoms SC to HG, Journal of Chemical Physics 82 (1985) 270–283.
[73] S. Miertus, E. Scrocco, J. Tomasi, Electrostatic interaction of a solute with a continuum. A direct utilizaion of AB initio molecular potentials for the prevision of solvent effects, Chemical Physics 55 (1981) 117–129.
[74] B. Keita, I.M. Mbomekallé, L. Nadjo, R. Contant, Compared Behaviours of Dawson-Type Tungstodiarsenates and–diphosphates, European Journal of Inorganic Chemistry 2 (2002) 473–479.
[75] X. López, J.J. Carbo, C. Bo, J.M. Poblet, Structure, properties and reactivity of polyoxometales: a theoretical perspective, Chemical Society Reviews 41 (2012) 7537–7571.